Available online at www.sciencedirect.com
SCIENCE DIRECT®
Chemical Physics Letters 408 (2005) 134–138
CHEMICAL PHYSICS LETTERS
www.elsevier.com/locate/cplett

The contact conductance on a molecular wire

S. Stojkovic [a,*], C. Joachim [a], L. Grill [b], F. Moresco [b]

[a] The NanoScience Group, CEMES/CNRS, 29 Rue J. Marvig BP 94347, Toulouse, France
[b] Institut für Experimentalphysik, Frei Universitat Berlin, Arnimallee 14, D-14195 Berlin, Germany

Received 21 December 2004; in final form 8 March 2005
Available online 27 April 2005

Abstract

On a metal–molecule–metal nanojunction, the scanning tunneling microscope (STM) scans at the precise location of the electronic metal–molecule interaction permit a measurement of the contact conductance G_0. The conversion curve between the change in the STM contrast Δh due to this interaction and G_0 is presented for a series of conjugated molecular wires. At chemisorption distances, the two-valued character of the $G_0(\Delta h)$ function is discussed, indicating experimental ways to evaluate G_0 as a function of Δh for different metal–molecule interaction ranges.

Molecular wires have attracted large interest due to their possible applications in nano-electronics [1,2]. A large variety of molecular wires have been synthesized and studied experimentally as well as theoretically to understand the conduction mechanisms supported by their molecular orbitals [3]. In a 'metal–molecular wire–metal' device, the molecular wire introduces an electronic coupling between the two electrodes. As a result, electrons are transferred from one electrode to the other through the molecular wire. The low voltage conductance of this device is given by [1,4]

$$G(E_f) = G_0 e^{-\gamma(E)L}, \quad (1)$$

where L is the distance between the two electrodes. At the Fermi level E_f, $\gamma(E_f)$ is the tunnel inverse decay length of the tunnel process and G_0 the so-called contact conductance of the molecular wire. $\gamma(E_f)$ is an intrinsic parameter of the molecular wire depending on its HOMO–LUMO gap and on the effective mass of the tunneling electrons [5]. G_0 characterizes how both ends of the molecular wire are interacting electronically with the surface of the metal electrodes. The difference (if any) between L and the molecular wire length is taken into account in G_0.

Using a scanning tunneling microscope (STM), γ can be measured by scanning along the molecular wire [6]. We have recently proposed to evaluate the effective electronic interaction α between the end of a molecular wire and its pad (and therefore G_0) by recording the change in the STM contrast at the metal surface location on the pads where the molecular wire ends [7–9].

At this location, the STM contrast change results in a 'contact bump' of height Δh relative to the same metal surface without the molecule. This is due to an increase of the tip apex end atom to surface electronic coupling through the end part of the molecular wire contacting the pad as illustrated in Fig. 1. Both the longitudinal tunnel barrier from the pad to the interior of the molecular wire and the vertical tunnel barrier from the tip apex to the surface of the pad are depending on α: G_0 is proportional to α^2 for a symmetric contacting (see Fig. 1a) and the intensity of the vertical STM current to $\alpha\beta$ with β the tip apex to molecular wire electronic coupling. Therefore, a constant current STM scan at the contact location open the way to evaluate α. The Δh value was measured on a series of Lander molecules [7–9] and on a Cu phtaolcyanine molecule manipulated

* Corresponding author. Fax: +33 (0) 5 62 2579 99.
E-mail address: stojkov@cemes.fr (S. Stojkovic).

0009-2614/$ - see front matter © 2005 Elsevier B.V. All rights reserved.
doi:10.1016/j.cplett.2005.04.015

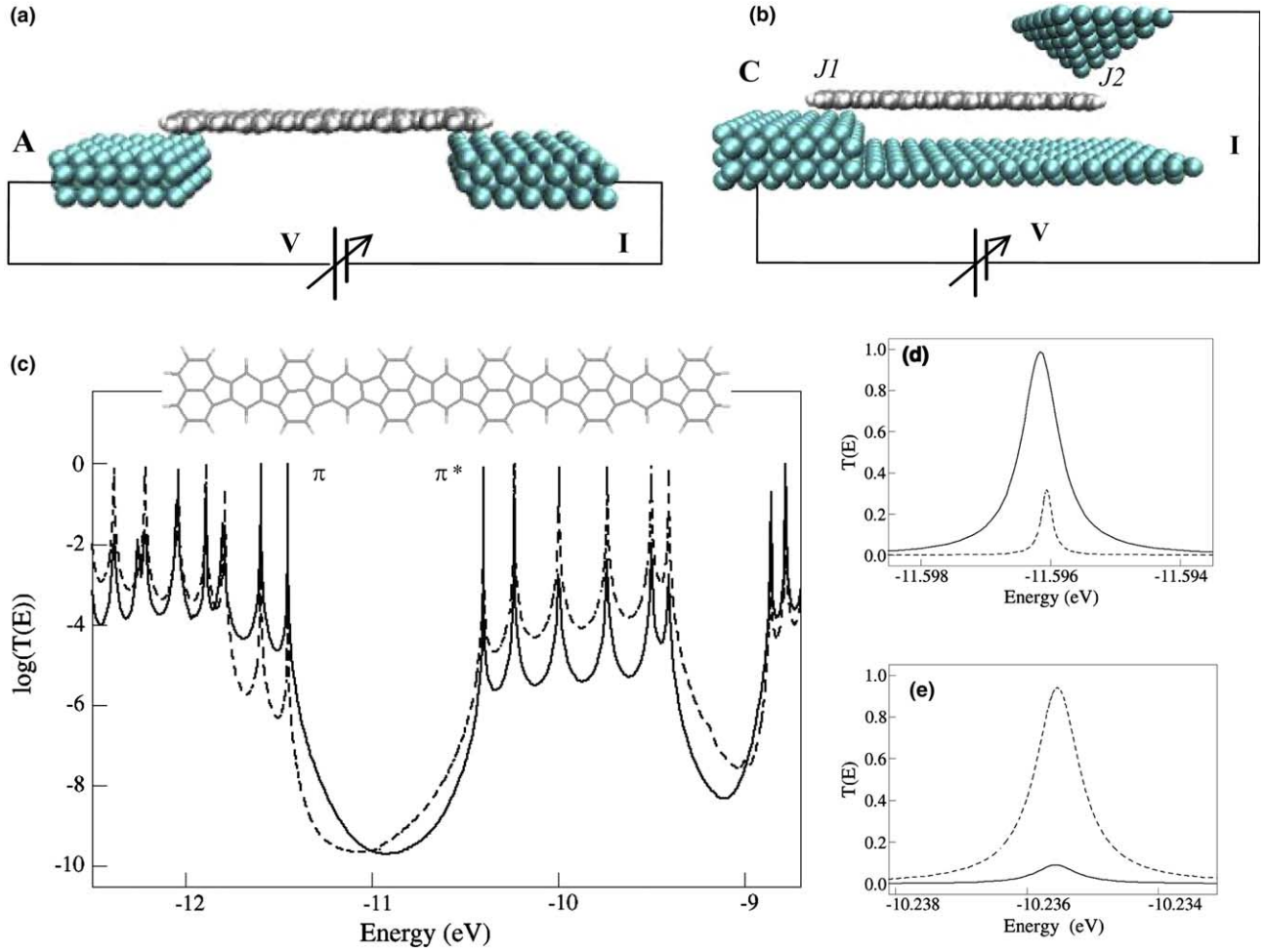

Fig. 1. Two different set-ups for measuring the conductance of a molecular wire. (a) A planar metal–molecular wire–metal junction (set-up A). (b) An STM set-up (C) where one end of the molecular wire is interacting with a step edge on the Cu(1 1 0). (c) Electronic transparency $T(E)$ spectra for set-up A (dashed lines) and set-up C (full line) calculated for $z = 3.5$ Å. For reference, the HOMO − 1 (d) and LUMO + 1 (e) resonances are presented for the two set-ups A (dashed lines) and C (solid lines). The considered molecular wire is made of 5 unit cells of the molecular board of the Lander molecule series [8,9].

to interact with two gold atomic wires [2]. The correspondence between G_0 and Δh through α is very useful for optimizing the end position of a molecular wire relative the atomic surface structure of the metal electrode [10]. For example, α is depending on the width of the pad and on electronic density of states at the surface of this pad.

In this Letter, we present and discuss the relationship between Δh and G_0 for a given family of conjugated molecular wires. First, $G_0(\Delta h)$ is calculated and discussed for a series of molecular wires as a function of the distance z between the molecular wire end and the metal surface. Then, Δh is calculated as a function of z taking into account that Δh is L independent (like G_0). Finally, the relation between G_0 and the electronic interaction Γ between the molecular wire and the metal surface is discussed.

For measuring G, the ideal experimental set-up A is presented in Fig. 1a. The molecular wire is similarly adsorbed at the end of two atomically clean metallic electrodes. According to (1), G_0 is evaluated by performing such a measurement on a series of molecular wires of different lengths to separate the exponential variation from the contact contribution [11]. In set-up C (Fig. 1b), the molecular wire is adsorbed at one end on the edge of an atomically defined step edge of a metal surface. This first metal–molecule junction *J1* is identical to those of set-up A. The second junction *J2* is realized with the metallic apex of an STM tip. Experimentally, the STM tip is scanned along the molecular wire and over the metal–molecule junction *J1* to measure Δh relative to a step edge without a molecule [6–8]. From this measurement, G_0 is evaluated with the advantage of using only one molecule and not a series of different lengths as in set-up A.

A typical electronic transmission coefficient spectrum $T(E)$ through a molecular wire is presented in Fig. 1c for the two set-ups. The molecular wire is made of the same

unit cells as the board of the Lander series [7,8]. $T(E)$ was calculated using the elastic scattering quantum chemistry (ESQC) technique [12]. In ESQC, the scattering matrix describing the metal–molecular wire–metal device is obtained from a semi-empirical extended Hückel mono-electronic Hamiltonian taking into account all the valence orbitals of the molecular wire and the valence atomic orbitals of each metal atom in the junction [12]. In ESQC, the effective Hamiltonian and propagator techniques ensure the perfect matching and self-energy between the junction and the semi-infinite metal periodic parts of the device in a multi-channel approach. In agreement with our recent experiments [8,9], a Cu(1 1 0) surface was chosen and the tip apex of the STM was supposed to be terminated by a small copper cluster.

The two $T(E)$ spectra presented in Fig. 1c are almost identical because the tip apex distance and position at the molecular wire were chosen to compensate the asymmetry between *J1* and *J2*. The tip apex is positioned in the center of the naphthalene end of the wire and the tip apex end atom height is 3 Å relative to the molecular wire. Each spectrum consists of characteristic resonant peaks corresponding to the π and σ molecular orbitals of the molecular wire. The large HOMO–LUMO π–π* gap is clearly visible. From these spectra and using the generalized Landauer formula [13], the multi-channel low voltage G of the devices in Fig. 1 was calculated as a function of the number of unit cells included in the molecular wire and of the distance z between the end of the molecular wire and the Cu(1 1 0) surface electrode.

According to (1) and after checking the exponential variation of G for each z value, G_0 was calculated as a function of z (Fig. 2). For set-up C, the tip apex to molecular wire end distance is the same as in Fig. 1. In both cases A and C, there is a large G_0 variation as a function of z because the electronic interaction between the molecular wire and the metal surface decreases exponentially with the distance. There is also an apparent saturation of G_0 when approaching chemisorption distances. At these small z values, the strong molecular orbital mixing between the molecular wire end and the surface states favors a large G_0. But such a large interaction also modifies locally the electronic structure of the metal surface. This increases the reflection coefficient of the metal electrons at the metal–molecule junction compared to the periodic electronic structure on the metal electrodes away from the junctions. This effect has a large influence on Δh as discussed hereafter.

The G_{0C} contact conductance of set-up C is combining the z dependence of two different metal–molecule junctions: *J1* at the metal step edge and *J2* between the tip apex and the other end of the molecular wire. This device asymmetry explains the large difference between G_{0A} and G_{0C}. The combination of this asymmetry in G_{0C} originates from the fact that in a first approximation the electronic transparency of a molecular device is proportional to the square of the electronic coupling introduced by the molecule between the two metallic electrodes [5]. At low coupling values, the resulting electronic coupling of two coupling in series is the renormalized product of these two [14]. Therefore, when a set-up B (see Fig. 2) has a symmetric contact arrangement (contact conductance G_{0B}) and a set-up D (see Fig. 2) has a two tip apex symmetric contact arrangement (contact conductance G_{0D}), the conductance G_{0C} of set-up C reflecting a type B contact on one side and a type D on the other side is given by

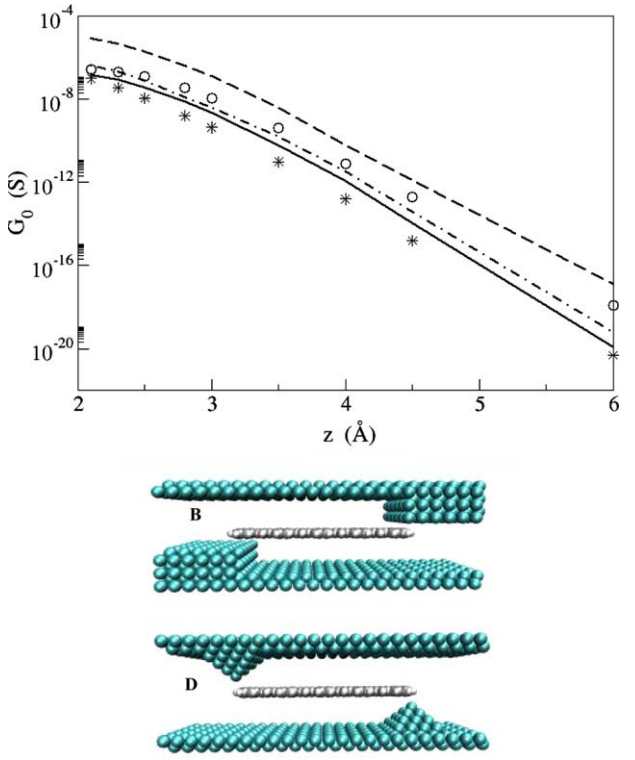

Fig. 2. Variation of the contact conductance as a function of the distance z between the molecular wire ends and different contact pads. G_{0A} and G_{0C} for set-ups A and C are indicated by dash and point-dash curves, respectively. G_{0B} and G_{0D} for set-ups B and D are indicated by circles and stars, respectively. The superposition law (2) leads to the solid curve. The set-ups A and C are defined in Fig. 1 and the set-up B and D are presented at the bottom of this figure.

$$G_{0C} = \sqrt{G_{0B} G_{0D}}. \quad (2)$$

Using z to tune the electrode–molecule interaction, we have calculated the contact conductance of set-ups B and D as presented in Fig. 2. The superposition rule (2) works well as compared to the standard superposition rule of adding the contact resistances $1/2G_{0B}$ and $1/2G_{0D}$ arranged in series in a circuit to get G_{0C} starting from G_{0B} and G_{0D}.

The saturation effect in $G_0(z)$ at small z is better observed by calculating Δh as a function of z because at the contact location the vertical tip apex to metal surface

tunneling intensity through the molecular wire end is very sensible to any local change of the metal density of states. To obtain Δh for set-up C, the ESQC program was used in its STM version by scanning at constant current along the molecular wire junction with the STM tip. The STM contrast increase Δh is obtained by comparing the two scans with and without the molecular wire positioned at the step edge in set-up C. The calculations were done only for a molecular wire of three unit cells, since we have first checked that-like $G_0 - \Delta h$ does not depend on the wire length. In Fig. 3, $\Delta h(z)$ is presented together with an example of a calculated STM scan along the molecular wire.

In contrary to the $G_{0C}(z)$ saturation shown in Fig. 2, the $\Delta h(z)$ curve in Fig. 3 shows a distinct maximum and decreases when approaching chemisorptions distances below 2.6 Å. This is due to the same induced chemisorption modification of the surface local density of state as discussed above. At *J1*, the vertical STM tunnel barrier is more sensible to this effect than the horizontal one. In the calculations, we can artificially re-enforced this effect by slightly contracting the Slater exponent of the atomic Cu 4s orbital describing the electronic structure of the copper atoms located directly under the end of the molecular wire. This contraction reduces the molecular wire–surface electronic interaction and a Δh increase results at chemisorption distances. Δh is also very sensible to the exact position of the molecular wire end at the edge of the electrode. A maximum $\Delta h = 93$ pm is calculated for $z = 2.7$ Å in a top adsorption geometry while for a bridge adsorption site $\Delta h = 87.5$ pm. At $z = 3.5$ Å, a $\Delta h = 70$ pm is calculated in agreement with the experimental Δh of a single Lander molecule adsorbed on a nanowire in a tilted configuration [8].

We have also studied how the width of each resonance peak in the $T(E)$ spectra (Fig. 1c) is changing with z. As an example, the peak shape of both HOMO − 1 and LUMO + 1 were calculated with the tip apex located exactly above *J1* in set-up C. A standard Lorentzian resonance shape is found and for example the effective half width Γ of the HOMO resonance decreases exponentially with a z increase (Fig. 4). Γ gives the electronic interaction between the metal surface and the molecular orbitals with a large weight on the carbon atoms located at the end of the molecular wire. At *J1*, the vertical tip apex metal surface tunnel barrier through the molecular wire end is controlled by this interaction. At chemisorption distances, Γ is small compared to the one usually obtained with a conjugated molecule completely chemisorbed on a metal surface. In fact, only a small part of the molecular orbitals are interacting with the metal surface in set-up C. For comparison, Γ was also calculated as a function of z when the full molecular wire is interacting with a flat Cu(1 1 0) surface (Fig. 4).

Combining the curves in Figs. 2 and 3 gives the conversion curve between Δh and G_0 in Fig. 5a. To plot this curve, we have first used Eq. (2) to separate the contribution of the 'tip apex–molecular wire end' contact from the one between the step edge and the other end of the molecular wire. For small Δh values, G_0 can be unambiguously determined as shown in Fig. 5a. For Δh values larger than 70 pm, two G_0 values are corresponding to the same Δh. This comes from the fact that the vertical STM tunnel current at the contact location is very sensitive to the local electronic change induced by the molecule on the metal surface state. As presented in Fig. 5b,

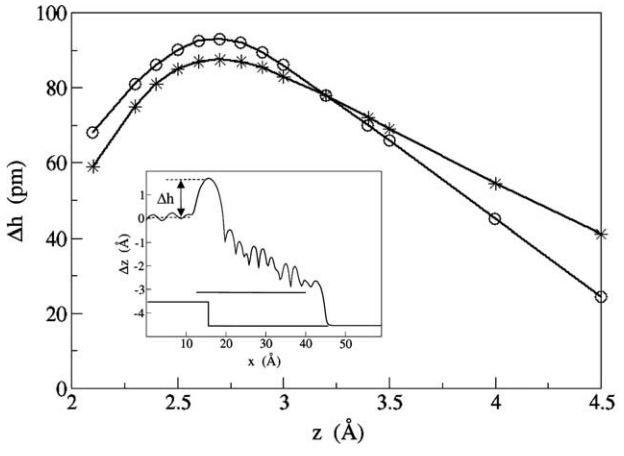

Fig. 3. Bump height Δh variation as a function of the distance z between the molecular wire and the step edge. The curve with circles was calculated for a top adsorption site while the curve with stars corresponds to a bridge adsorption site. The inset shows an example of a calculated constant current STM scan along the x direction of a molecular wire connected to the surface step (as is schematically presented at the bottom of this inset) in a set-up C for $z = 2.8$ Å.

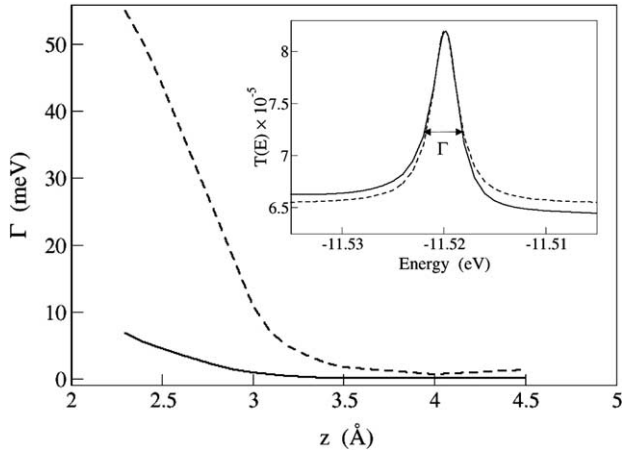

Fig. 4. The interaction energy Γ between the molecular wire end and the step edge in set-up C calculated as the half-width peak height of the HOMO resonance as a function of the distance z. The solid curve is the interaction at the step edge while the dashed curve is calculated for a molecule fully adsorbed on the Cu(1 1 0) surface (with the tip positioned above the center of molecule). As one example for $z = 2.3$ Å in the inset the $T(E)$ resonance (solid curve) is fitted by a Lorentzian (dashed curve).

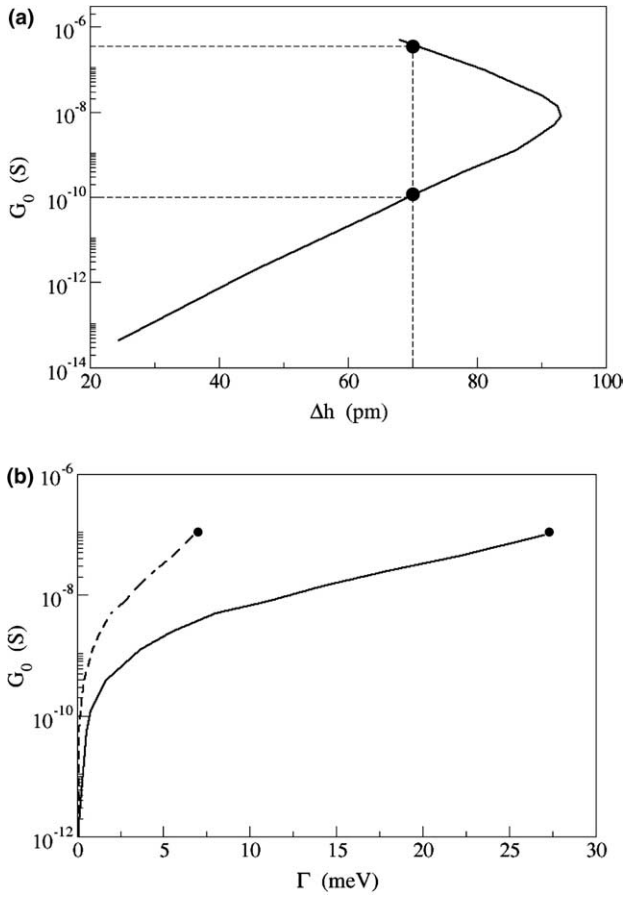

Fig. 5. (a) Conversion curve between the contact bump height Δh and the contact conductance G_0. (b) Conversion curve between G_0 and Γ LUMO (solid curve) and HOMO (dashed curve). Notice that one can also get the conversion curve between Δh and the electronic interaction energy Γ. In (a) a measured $\Delta h = 70$ pm can be attributed either to a 100 pS or 500 nS contact conductance (marked by dashed lines). In (b) solid dots indicate the distance where the chemisorption is reached.

G_0 is a monotonous function of Γ. Therefore, an experimental way to lift up the indetermination of G_0 as a function of Δh is to measure the Lorentzian width of the HOMO and LUMO molecular orbitals by recording a STM spectrum at the *J1* contact location. A width well below $\Gamma = 50$ meV will be an indication of the physisorption state of the molecular wire end at the step edge while a larger value indicates a chemisorption state.

One can apply the Fig. 5a curve to our recent contact experiments performed in atomically clean conditions where the measured Δh ranges between 20 and 70 pm [7–9]. According to the Fig. 5a curve, these values correspond to a contact conductance between 10^{-13} and 10^{-10} Siemens, respectively, if one remains on the lower part of this curve. But the experimental $\Delta h = 70$ pm value can also be attributed to a complete chemisorption of the end of the molecular wire at the step edge. In this case, one gets a large contact conductance in the range of 5×10^{-7} Siemens. These values must be compared to the 7.7×10^{-5} Siemens contact conductance of a 1D ballistic wire (where $\gamma = 0$ in (1)) contacted to a metallic pad as measured with a single wall carbon nanotube [15] or to the 3.85×10^{-5} Siemens contact conductance of an Au atomic metallic chain [16].

In conclusion, the change in the scanning tunneling microscopy contrast measured at the location of a metal–molecular wire junction can be used as a measure of the metal–molecular wire–metal junction contact conductance. It is not necessary to perform multiple measurements of the conductance of this device for different molecular wire lengths to get its contact conductance. Our detailed study of the conversion curve between the contact bump height and the contact conductance points out that the price to pay for this reduction of the experimental effort is a two-valued $G_0(\Delta h)$ curve at large Δh values. This indetermination of G_0 can be nicely lifted up by measuring the width of the molecular orbital resonance at the same location as the Δh measurements. Finally, there is a need to design very efficient contacting end groups for increasing the contact conductance up to the micro Siemens regime.

Acknowledgments

Founding by the European IST project CHIC, by the European RTN network AMMIST and by the Volkswagen Foundation project 'Single Molecule Synthesis' is gratefully acknowledged.

References

[1] C. Joachim, J.K. Gimzewski, A. Aviram, Nature 48 (2000) 541.
[2] M. Reed, Proc. IEEE 87 (1999) 652.
[3] C. Joachim, M.A. Ratner, Nanotechnology 15 (2004) 1065.
[4] M. Magoga, C. Joachim, Phys. Rev. B 56 (1997) 4722.
[5] A. Lahmidi, C. Joachim, Chem. Phys. Lett. 381 (2003) 335.
[6] V.J. Langlais, R.R. Schlittler, H. Tang, A. Gourdon, C. Joachim, J.K. Gimzewski, Phys. Rev. Lett. 83 (1999) 2809.
[7] F. Moresco, L. Gross, M. Alemani, K.H. Rieder, H. Tang, A. Gourdon, C. Joachim, Phys. Rev. Lett. 91 (2003) 036601.
[8] L. Grill, F. Moresco, P. Jiang, C. Joachim, A. Gourdon, K.H. Rieder, Phys. Rev. B 69 (2004) 035416.
[9] L. Grill, F. Moresco, K.H. Rieder, S. Stojkovic, A. Gourdon, C. Joachim, Nano Lett. (2005), (in press).
[10] M. Magoga, C. Joachim, Phys. Rev. B 59 (1999) 16011.
[11] L.A. Bumm, J.J. Arnold, T.D. Dunbar, D.L. Allara, P.S. Weiss, J. Phys. Chem. B 103 (1999) 8122.
[12] P. Sautet, C. Joachim, Chem. Phys. Lett. 185 (1991) 23.
[13] M. Büttiker, Y. Imry, R. Landauer, S. Pinhas, Phys. Rev. B 31 (1985) 6207.
[14] P. Sautet, C. Joachim, J. Phys. C 21 (1988) 3939.
[15] S.J. Tans, M.H. Devoret, H. Dai, A. Thess, R.E. Smalley, L.J. Geerligs, C. Dekker, Nature 386 (1997) 474.
[16] H. Ohnishi, Y. Kondo, K. Takayanagi, Nature 395 (1988) 780.